Computers and Electrical Engineering 36 (2010) 1193–1201

Contents lists available at ScienceDirect

Computers and Electrical Engineering

journal homepage: www.elsevier.com/locate/compeleceng

Technical Communication

Infrared small target enhancement and detection based on modified top-hat transformations ☆

Xiangzhi Bai *, Fugen Zhou

Image Processing Centre, Beijing University of Aeronautics and Astronautics, Beijing 100191, China

ARTICLE INFO

Article history:
Received 17 June 2009
Received in revised form 7 May 2010
Accepted 25 May 2010
Available online 23 June 2010

Keywords:
Top-hat transformation
Target enhancement operation
Infrared small target
Target enhancement
Target detection

ABSTRACT

To simply and efficiently enhance and detect infrared small target, a new algorithm through target enhancement by using modified top-hat transformations is proposed. Firstly, the modified top-hat transformations following the property of small target region are discussed, which could efficiently extract the possible target and dark regions. Secondly, the potential target regions are enhanced by using a target enhancement operation which is formed through enlarging the contrast between bright and dark regions using the modified top-hat transformations. Finally, an iterative thresholding method is used to automatically detect the target region. Various infrared images embedded with small targets are used to verify the efficiency of the algorithm, and experimental results show that our algorithm is very efficient.

1. Introduction

Infrared small target detection is a crucial technique for military, aeronautics and astronautics applications. Because the target is far away from the imaging equipment and moving fast, the small target in infrared image usually has the properties of dim target intensity, clutter background and unavailable shape information [1–12]. These properties heavily increase the difficulty of target detection. To efficiently detect the infrared small target, the dim target in clutter background should be enhanced. Infrared small target detection through target enhancement has attracted increasing interests over the last few years. Many target enhancement algorithms are proposed to detect infrared small targets, including filter-based algorithms [1–3], wavelet based algorithms [4], mathematical morphology based algorithms [5–10] and some other methods by using intelligent tools [11–14] or motion properties of target [15,16].

Filter-based algorithms enhance small target through suppressing the clutter background by using filters to filter the possible target regions. To be simple and efficient, various filters have been designed, such as kernel filters [1], max-mean filter [2], max-median filter [2] and adaptive lattice algorithm [3]. Although the filters-based algorithms are simple or efficient in some cases, they can not perform well if the target is dim and clutter is heavy. Wavelet based algorithms [4] enhance small target through extracting the different properties between the target region and clutter background. But, because the target is dim and small, wavelet based algorithms can not efficiently extract the properties of target region in some cases. The algorithms using intelligent tools [11–14] perform well if the training set they needed is well organised. But, it is not usually very easy to obtain a good training set for infrared small target. Algorithms of detecting dim small target using motion properties [15,16] need multi consecutive images. However, in some cases, the multi consecutive images could not be easily obtained. Mathematical morphology based algorithms [5–10] mainly use top-hat transformation to suppress clutter background and

☆ Reviews processed and proposed for publication to the Editor-in-Chief by Associate Editor Dr. Sahin.
* Corresponding author. Tel.: +86 1082338048.
E-mail address: jackybxz163@163.com (X. Bai).

0045-7906/$ - see front matter © 2010 Elsevier Ltd. All rights reserved.
doi:10.1016/j.compeleceng.2010.05.008

enhance small target. But, top-hat transformation is sensitive to dim target and clutter background. Finding efficient structuring element used in top-hat transformation is one way to improve the performance of top-hat transformation, but the improvement is limit.

To simply and efficiently enhance and detect infrared dim small target embedded in clutter background, a new algorithm through target enhancement by using modified top-hat transformations is proposed. Firstly, modified top-hat transformations following the properties of small target region are discussed. Secondly, a target enhancement operation is formed based on modified top-hat transformations and used to enhance infrared small target. Finally, the enhanced small target is automatically detected by using an iterative thresholding method. Experimental results of various infrared images embedded with small targets verified that our algorithm was efficient. Section 2 gives a brief description of top-hat transformation. Section 3 demonstrates the target enhancement operation based on the modified top-hat transformations. Section 4 addresses the iterative thresholding method for target detection. Section 5 discusses the experiments and Section 6 concludes the paper.

2. Top-hat transformation

Mathematical morphology is proposed by Matheron and Serra and extended to image analysis [17]. All of the mathematical morphological operations work with two sets. One set is the original image to be analysed and the other set is called structuring element.

For gray-scale image, the dilation, erosion, opening, closing, white top-hat transformation (WTH) and black top-hat transformation (BTH) of $f(x, y)$ by flat structuring element $B(i, j)$, are defined as follows [17]

$$f \oplus B = \max_{i,j}(f(x-i, y-j)) \tag{1}$$

$$f \Theta B = \min_{i,j}(f(x+i, y+j)) \tag{2}$$

$$f \circ B = (f \Theta B) \oplus B \tag{3}$$

$$f \bullet B = (f \oplus B) \Theta B \tag{4}$$

$$\mathrm{WTH}(x,y) = f(x,y) - f \circ B(x,y) \tag{5}$$

$$\mathrm{BTH}(x,y) = f \bullet B(x,y) - f(x,y) \tag{6}$$

Opening smoothes bright regions of image and closing smoothes dark regions. So, following expressions (5) and (6), WTH finds out bright regions in f, and BTH gives out dark regions [17]. Then, they can be used to detect the potential small target region. But, because they are sensitive to the clutter variation and dim target intensity [5–7], top-hat transformations are inefficient way when the clutter is heavy and target is dim.

3. Target enhancement operation

3.1. Modified top-hat transformation

Expressions (5) and (6) indicate that, all the regions the gray-values changed after opening or closing operation will have outputs in WTH or BTH. Unfortunately, most of them correspond to clutter background. And those regions will heavily increase the number of false alarms and therefore the difficulty of target detection.

Infrared image embedded with a small target can be modelled as follows [1,5–7,9,19]:

$$f(r,k) = S(r,k) + f_b(r,k) + n(r,k), k = 0, 1, 2, \ldots \tag{7}$$

where $r = (x, y)$ is the spatial coordinate of image f; k is the sampled time; $f_b(r, k)$ is the clutter background and $n(r, k)$ is the noise at sampled time k; $S(x,y)$ is the target intensity. The spatial target signature is an optical blur dominated by the optics point spread function and can be well modelled by the 2 D Gaussian shape [1,5–7,9,19],

$$S(x,y) = \exp\{-[(x/\sigma_x)^2 + (y/\sigma_y)^2]/2\} \tag{8}$$

where σ_x and σ_y are the horizontal and vertical extent parameters, respectively.

Expressions (7) and (8) indicate one important property of small target region: the gray-values of target region are usually larger than the gray-values of the surrounding background. In another way, opening operation in WTH is usually used to smooth bright region. Then, after opening, the gray-value of bright region will be changed. Therefore, only the regions whose gray-value changes (denoted by *GVC*) after opening operation are larger than a certain value may be the potential target regions [9]. In light of this, a judging value can be imported into the original top-hat transformation to identify the potential target regions.

Following the definition of opening in expression (3), the erosion operation in opening takes the minimum value in region B to replace the gray-value of the corresponding pixel in f[17]. All the values in region B after erosion form a set denoted by *VB*. The following dilation operation in opening takes the maximum value in *VB* to replace the gray-values of corresponding

pixels. So, the *GVC* of each pixel after opening is the difference of original gray-value of current pixel and the maximum value of *VB* [9], that is:

$$GVC(x,y) = f(x,y) - \max(VB) \tag{9}$$

Since the gray-values of target region are usually larger than the gray-values of surrounding background, all the values of *VB* are smaller than the gray-values of target region. Then, *GVC* of the target region will be a positive value. So, if the judging value, denoted by *t*, is smaller than *GVC*, the corresponding pixel will be in target region. Therefore, the judging value *t* can be calculated following the *GVC* after opening operation [9]. To find the judging value reasonably and easily, a procedure of the calculation of *t* is performed as follows.

Step 1: Select a $L \times L$ window *w*, locate the centre of *w* at each pixel of *f*;
Step 2: Find the maximum (*wMax*) and minimum (*wMin*) values of the pixels in *w*;
Step 3: Calculate the difference of *wMax* and *wMin* for each pixel, and all of these differences form a new image which is the gray change map and denoted by *GCM*;
Step 4: $t = m + \delta \times \sigma$, where *m* and σ are the mean and standard deviation of *GCM*. δ is an adjustable parameter, and should be selected according to the intensity of target. If the target is dim, δ should be small. Otherwise, δ should be large. In most cases, δ can be selected in [0, 10.0].

The size of *w* should be smaller than the size of target region, which can be easily obtained from the prior knowledge of target. In this case, the values of *GCM* can be divided into three classes: the clutter background, the brim of target region and the target region. The output of the clutter background in *GCM* is small, but may exceed the *GVC* of these regions because of the clutter background, thus these clutter background are suppressed. The brim of target region has a large output in *GCM* because the gray-values of target region is larger than the gray-values of surrounding clutter background, which marks out the target region and corresponds to target region. The output of target region in *GCM* is small because of the consistency of the gray in target region, which is smaller than the *GVC* of target region. All of these mean that a judging value which is smaller than the large value of *GCM* and larger than most of the smaller value of *GCM* can mark out potential target region and suppress clutter background.

In another way, *t* is larger than *m*, which exceeds the *GVC* of the most of clutter background and thus these clutter background will be suppressed. Meanwhile, *t* is smaller than the large value of *GCM*, which will not exceed the *GVC* of target region and thus the target region will be remained. Then, *t* calculated from *GCM* is a reasonable value and can be imported into original top-hat transformation to identify potential target region.

By using *t*, the modified white top-hat transformation (MWTH) [9] could be expressed as follows:

$$\mathrm{MWTH}(x,y) = \max(f(x,y) - f \circ B(x,y), t) - t \tag{10}$$

Similarly, the modified black top-hat transformation (MBTH) [9] could also be expressed as follows:

$$\mathrm{MBTH}(x,y) = \max(f \bullet B(x,y) - f(x,y), t) - t \tag{11}$$

The size of structuring element should be larger than the largest target region. MWTH indicates that, not all of the changed regions are potential target regions, but the brighter regions whose *GVC* are larger than *t*. *t* is larger than *m*, which means *t* is larger than most of the *GVC* of clutter background. Then, most of clutter background will be suppressed because of *t* in MWTH. Heavy clutter results in a larger σ, and therefore a larger *t*. Then, more clutter will be suppressed. Consequently, the importing of *t* which is calculated following the property of small target region largely improves the efficiency of MWTH for real potential target region identification and decreases the number of false alarms [9]. Also, the importing of *t* in MBTH has the similar property to MWTH for real dark region identification.

Obviously, if $t = 0$, MWTH and MBTH will degenerate as:

$$\mathrm{MWTH}(x,y) = \max(f(x,y) - f \circ B(x,y), 0) - 0 = f(x,y) - f \circ B(x,y) = \mathrm{WTH} \tag{12}$$

$$\mathrm{MBTH}(x,y) = \max(f \bullet B(x,y) - f(x,y), 0) - 0 = f \bullet B(x,y) - f(x,y) = \mathrm{BTH} \tag{13}$$

So, WTH and BTH are the specific cases of MWTH and MBTH.

3.2. Target enhancement operation

MWTH finds out potential target regions and MBTH gives out dark regions. So, the target enhancement operation (TEO) can be defined as follows:

$$ef(x,y) = \alpha * f(x,y) + \beta * \mathrm{MWTH}(x,y) - \gamma * \mathrm{MBTH}(x,y) \tag{14}$$

where α, β and γ are positive and adjustable coefficients. Expression (14) shows that smaller α, larger β and larger γ result in a stronger intensity of target region and a lower intensity of clutter background in *ef*. In most cases, $\alpha \leqslant 1$, $\beta \geqslant 1$ and $\gamma \geqslant 1$. In TEO, the intensity of potential target region is increased and the intensity of dark region is decreased. Then, the contrast of bright region and dark region is strongly increased, and thus the potential target regions are largely enhanced after TEO.

4. Target detection

The enhanced image after TEO has large number of pixels with small gray values and the histogram is usually uni-mode. Then, it is not very easy to find an appropriate threshold for target detection. To decrease the possible false alarms in final binary target image and threshold the image automatically, an iterative thresholding [18] algorithm is used in this paper. The procedure of the algorithm is demonstrated below. However, because the target is apparently enhanced, the target regions are very bright after TEO. So, the target could also be efficiently detected through a threshold generated by the prior knowledge of target or some other thresholding algorithms.

Step 1: Calculate the mean or the half of the maximum gray value of *ef* as the initial value of the threshold, denoted by T_h.
Step 2: Divide *ef* into two classes according to the threshold T_h: target and background, denoted by *Tar* and *Bac*, respectively.
Step 3: Calculate the mean gray value of *Tar* and *Bac*, denoted by $mean_{up}$ and $mean_{down}$, respectively. The difference between $mean_{up}$ and $mean_{down}$ is defined by

$$diff = mean_{up} - mean_{down}. \tag{15}$$

Step 4: Calculate the new threshold of *ef* by the following expression:

$$T_n = (1 - 1/f(diff)) \times mean_{down} + (1/f(diff)) \times mean_{up} \tag{16}$$

where $f(diff) = \log_{10}(10 + \varepsilon \times diff)$. ε is a constant coefficient according to the image and varies following different images. The smaller the mean value of image is, the smaller the ε is. Generally, ε is selected from [0,10].
Step 5: Check if $T_n = T_h$, then the ultimate threshold of *ef* is $T_p = T_n$;

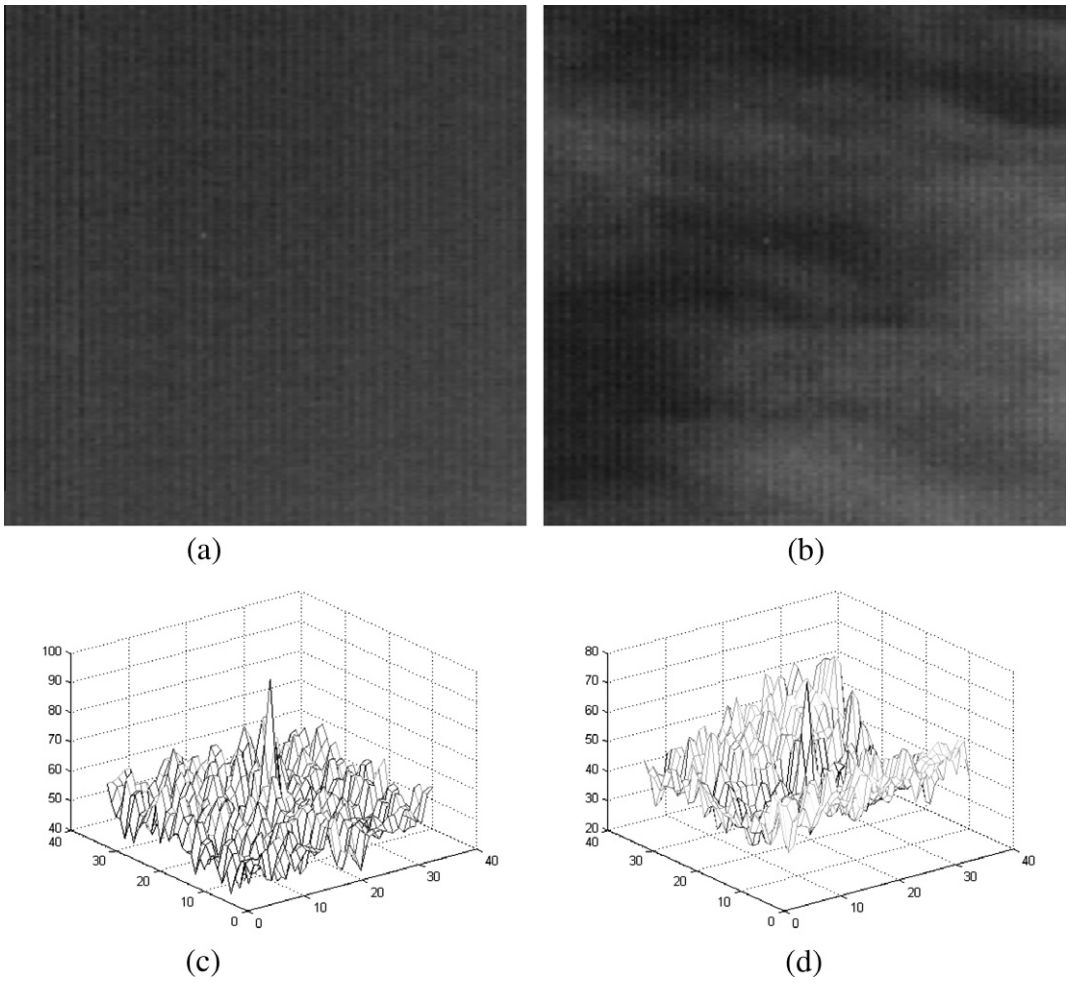

Fig. 1. Original infrared images with different clutter backgrounds: (a) sky clutter infrared image (LSBR = 0.5326); (b) cloud clutter infrared image (LSBR = 0.1206); (c) 3 D plot of the intensity of (a); (d) 3 D plot of the intensity of (b).

Otherwise, let $T_h = T_n$ and go to Step 2.

As the procedure indicates, more clutter with large gray-value results in a larger T_h, and leads to a small *diff* which is the difference of $mean_{up}$ and $mean_{down}$. Then, $f(diff)$ goes down, and T_n goes up following expression (16). Consequently, most of the clutter background with large gray-values is suppressed, and the false alarms are depressed. So, this iterative thresholding algorithm could automatically detect small target.

5. Experimental results

To verify the efficiency of the proposed algorithms, more than 200 images with different clutter backgrounds are used in this experiment. Experimental images are infrared images embedded with small targets. The clutter of images is heavy and the targets are very dim.

Table 1
Comparison of several small target detection methods.

Enhancement method	Fig. 1(a) (LSBR = 0.5326)		Fig. 1(b) (LSBR = 0.1206)	
	LSBR (db)	LSBR gain	LSBR (db)	LSBR gain
TEO	17.9596	17.4270	9.4058	9.2852
Top-hat transformation	0.5689	0.0363	0.5092	0.3886
Max-median (3 × 3)	4.1409	3.6083	2.9259	2.8053
Max-mean (3 × 3)	0.9035	0.3709	0.3756	0.2550
Max-median (5 × 5)	1.0890	0.5564	0.3342	0.2136
Max-mean (5 × 5)	1.3890	0.8564	0.7644	0.6438
U-kernal	5.9664	5.4338	2.7040	2.5834
E-kernal	5.7706	5.2380	2.8672	2.7466

Table 2
More comparison results on infrared small target images with different clutter backgrounds (LSBR).

Original images	1.6753	1.0049	0.6091	0.6870	0.0685	0.0421	0.5057	0.6199	0.2399	0.7572
TEO	16.5330	6.1546	3.3983	12.9207	3.1971	10.1564	11.3843	2.1956	9.9850	12.8915
Top-hat transform	6.6579	3.2356	0.9238	1.1359	1.1107	0.8355	1.0125	0.7277	0.7368	0.8785
Max-median (3 × 3)	3.5159	1.1297	1.8295	5.7222	2.4304	7.2882	7.9542	2.0171	4.7905	4.8146
Max-mean (3 × 3)	3.4330	1.5386	0.7458	1.3418	1.1374	1.6307	1.5162	0.7119	0.9800	0.8987
Max-median (5 × 5)	7.9922	3.5465	0.6134	0.9368	1.0782	1.5699	0.9902	0.7245	1.0265	0.8168
Max-mean (5 × 5)	6.8372	2.8320	1.2950	2.2165	1.3914	1.7774	1.7708	1.0608	1.5494	1.4632
U-kernal	4.6180	2.3970	1.9052	3.8870	1.9712	0.7988	2.1715	1.7426	1.4227	0.6365
E-kernal	4.5513	2.1023	1.8153	3.7015	2.0189	0.8065	2.1193	1.6892	1.3447	0.6153

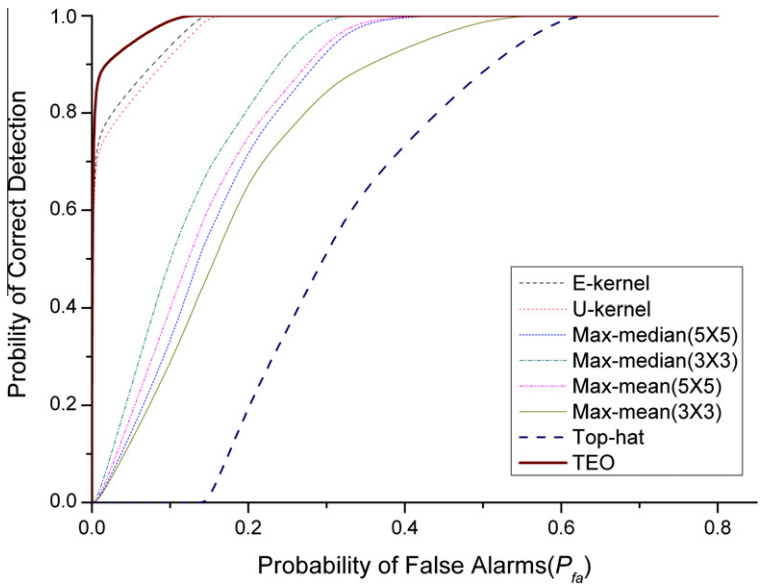

Fig. 2. ROC curves of different algorithms for infrared small target images with heavy clutter background.

5.1. Target enhancement experiment

To demonstrate the efficient property of TEO for small target enhancement, a measure LSBR [7,9,19] (Local Signal to Background Ratio) is used here to do the comparison.

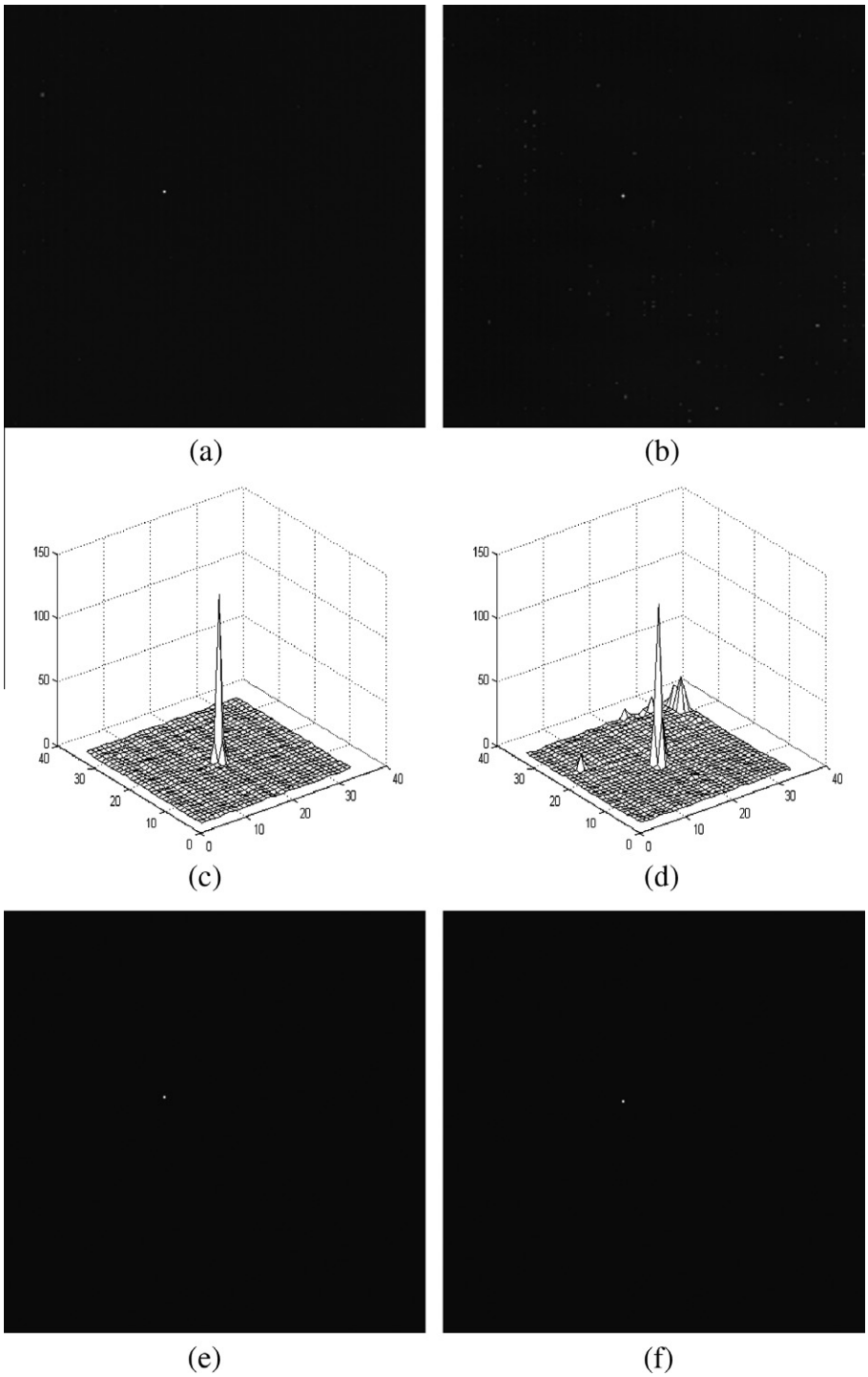

Fig. 3. Target enhancement and detection results: (a) enhancement result of Fig. 1a by using TEO; (b) enhancement result of Fig. 1b by using TEO; (c) 3 D plot of the intensity of (a); (d) 3 D plot of the intensity of (b); (e) detection result of Fig. 1a; (f) detection result of Fig. 1b.

$$\mathrm{LSBR} = 10\log\left\{\frac{1}{\sigma_b^2}\sum_{k=-W/2}^{W/2}\sum_{j=-W/2}^{W/2}[I(s-k,r-j)-m_b]^2\right\} \tag{17}$$

where σ_b^2 and m_b are the variance and mean of the background in the window described by the width and height W around the interest pixel (s, r), respectively. Smaller LSBR indicates a dimmer target and heavier clutter.

Two example images and the corresponding 3 D plots of the intensity of target region and surrounding background are shown in Fig. 1. LSBRs of the original images in Fig. 1 are small and the clutter is heavy. LSBRs of the target regions after various target detection methods are listed in Table 1. LSBRs of top-hat transformation are worse than most of the other methods because of heavy clutter and dim target intensity. Conversely, the effect of TEO is better than other methods no matter how heavy the clutter is.

Moreover, more than 200 infrared dim small target images with sky, cloud, sea and building clutter backgrounds are used in the experiments and most of the results show that TEO could efficiently enhance the infrared dim small targets embedded in different clutter backgrounds. Some more results are shown in Table 2. In Table 2, LSBRs of the dim small targets in original images and the result images after different methods are shown. Because the targets in original images are dim and the clutter is heavy. The LSBRs of the targets in original image are small. All the methods could enhance the dim targets, which results in larger LSBRs of the targets than the original image. However, the LSBRs of the targets in the result images of TEO are very larger than any other methods. This indicates that, the target enhancement performance of

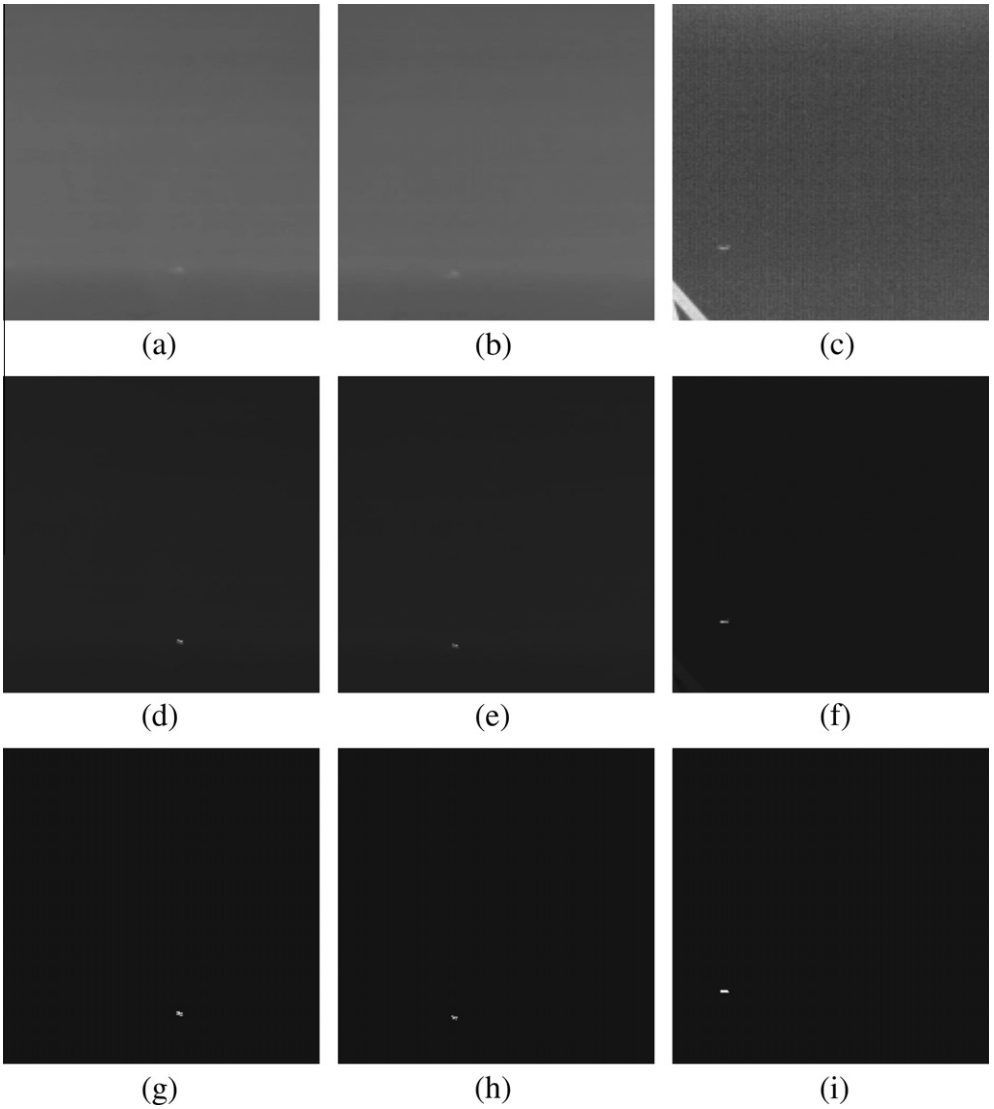

Fig. 4. Some more target enhancement and detection results: (a)–(c) original images; (d)–(f) enhancement results by using TEO; (g)–(i) detection results.

TEO is better than other methods. So, TEO could efficiently enhance infrared dim small target embedded in different clutter backgrounds.

5.2. Target detection experiment

To demonstrate the efficiency of our algorithm for small target detection, infrared images are used to generate the ROC curve plots [8] (Fig. 2). Fig. 2 shows that TEO can detect more accurate target than other methods according to the same P_{fa} (Probability of False Alarms). Moreover, ROC curve of TEO sharply approach one, which indicates a better performance for small target detection. Fig. 2 shows that because of the superiority of modified top-hat transformations for clutter suppression and target enhancement, TEO which is constructed from modified top-hat transformations could perform very well under different clutters for target detection.

Table 1 shows a better performance of Max-median than U-kernel and E-kernel, but ROC curves show a better performance of U-kernel and E-kernel. This indicates that these methods are un-robust. Different from these methods, TEO shows an efficient performance for target enhancement and detection in all the experiments, which means that TEO is efficient and robust for target enhancement and detection.

To directly show the efficient performance of our algorithm, the resulting image of Fig. 1 after TEO and the intensity of target region and surrounding background in 3 D plots are shown in Figs. 3(a)–(d). Most of the clutter is suppressed and the targets are apparently enhanced as shown in Figs. 3(a) and (d). So, the targets can be easily detected by threshold T_p (Figs. 3(e) and (f)).

To show the efficient performance of our algorithm on more images, three more infrared dim small target images and the enhancement and detection results are shown in Fig. 4. In Fig. 4, (a)–(c) are the three original infrared dim small target images. (d)–(f) are the enhanced results after TEO. (g)–(i) are the detection results of our algorithm. Because the targets are very dim and the images have different clutter backgrounds, the targets are almost embedded in the original images. But, after TEO, the dim targets are significantly enhanced and the clutter background is efficiently suppressed. Then, the targets are very bright. Therefore, the enhanced targets could be easily detected. All of the experimental results show that our algorithm could be efficiently used for infrared dim small target enhancement and detection.

The shape of structuring element used in this experiment is rectangle and the size is 5×5. $\delta = 1.0$, $\alpha = 0.1$, $\beta = 5.0$, $\gamma = 1.0$, $\varepsilon = 5.0$, $W = 33$. LSBRs of targets in experimental images are small and the clutter of images is heavy, which indicates that our algorithm could perform well even under the conditions of low target intensity and heavy clutter.

6. Conclusion

To simply and efficiently enhance and detect infrared dim small target embedded in clutter background, the modified top-hat transformations following the property of small target region are used to form a new target enhancement operation (TEO). Because of the importing of the property of small target into the modified top-hat transformations, TEO largely enhances small target and efficiently suppresses clutter background. Therefore, the target can be easily detected through an iterative thresholding method. Experiments show that our algorithm is very efficient than other methods. Moreover, our algorithm could also be used not only in infrared images.

Acknowledgment

We thank the reviewers for their very constructive comments. We also would like to thank Dr. Yan Li at Peking University, Beijing, China, for many helpful discussions and comments. This work is partly supported by the National Natural Science Foundation of China (60902056), Aeronautical Science Foundation of China (20090151007), China Scholarship Council and Innovation Foundation of Beijing University of Aeronautics and Astronautics for PhD Students.

References

[1] Leonov S. Nonparametric method for clutter removal. IEEE Trans Aerosp Electron Syst 2001;37(3):832–48.
[2] Deshpande SD, Er MH, Ronda V, Chan Ph. Max-mean and max-median filters for detection of small-targets. Proc SPIE 1999;3809:74–83.
[3] Ffrench PA, Zeidler JR, Ku WH. Enhanced detectability of small objects in correlated clutter using an improved 2-D adaptive lattice algorithm. IEEE Trans Image Process 1997;6(3):383–97.
[4] Arodz T, Kurdziel M, Popiela TJ, Sevre EOD, Yuen DA. Detection of clustered microcalcifications in small field digital mammography. Comput Methods Programs Biomed 2006;81:56–65.
[5] Zhang F, Li C, Shi L. Detecting and tracking dim moving point target in IR image sequences. Infrared Phys Technol 2005;46:323–8.
[6] Zeng M, Li J, Peng Z. The design of top-hat morphological filter and application to infrared target detection. Infrared Phys Technol 2006;48:67–76.
[7] Bai X, Zhou F, Xie Y. New class of top-hat transformation to enhance infrared small targets. J Electron Imaging 2008;17(3):0305011.
[8] Braga-Neto U, Choudhary M, Goutsias J. Automatic target detection and tracking in forward-looking infrared image sequences using morphological connected operators. J Electron Imaging 2004;13(4):802–13.
[9] Bai X, Zhou F, Jin T. Enhancement of dim small target through modified top-hat transformation under the condition of heavy clutter. Signal Process 2010;90:1643–54.
[10] Halkiotis S, Botsis T, Rangoussi M. Automatic detection of clustered microcalcifications in digital mammograms using mathematical morphology and neural networks. Signal Process 2007;87:1559–68.

[11] Jin X, Davis CH. Vehicle detection from high-resolution satellite imagery using morphological shared-weight neural networks. Image Vision Comput 2007;25:1422–31.
[12] Wang P, Tian JW, Gao CQ. Infrared small target detection using directional highpass filters based on LS-SVM. Electron Lett 2009;45(3):156–8.
[13] El-Napa I, Yang YY, Wernick MN, Galatsanos NP, Nishikawa RM. A support vector machine approach for detection of microcalcifications. IEEE Trans Med Imaging 2002;21(12):1552–63.
[14] Liu Z, Shen X, Chen C. Small objects detection in image data based on probabilistic visual learning. In: Proceedings of fourth international conference on machine learning and cybernetics. Guangzhou, China: 2005; p. 5517–21.
[15] Moon YS, Zhang TX, Zuo ZR, Zuo Z. Detection of sea surface small targets in infrared images based on multilevel filter and minimum risk Bayes test. Int J Pattern Recognit Artif Intell 2000;14:907–18.
[16] Cafer CE, Silverman J, Mooney JM. Optimization of point target tracking filters. IEEE Trans Aerosp Electron Syst 2000;36(1):15–25.
[17] Serra J. Image analysis and mathematical morphology. New York, USA: Academic Press; 1982.
[18] Bai X, Zhou F. Edge detection based on mathematical morphology and iterative thresholding. In: Proceedings of international conference on computational intelligence and security. Guangzhou, China: 2006; p. 1849–52.
[19] Soni T, Zeidler JR, Ku WH. Performance evaluation of 2-D adaptive prediction filters for detection of small objects in image data. IEEE Trans Image Process 1993;2(3):327–40.

Xiangzhi Bai received his B.S. degree from Beijing University of Aeronautics and Astronautics (BUAA) in 2003 and his Ph.D. from BUAA in 2009. He is currently a lecture of image processing center of BUAA. From 2007 to 2008, he was with the CSIRO Mathematical and Information Sciences, Sydney, Australia. His research interests include computer vision, image analysis, pattern recognition, and bioinformatics.

Fugen Zhou received his B.S. degree from Beijing University of Aeronautics and Astronautics (BUAA) in 1986 and his PhD from BUAA in 2006. His research interests include object recognition, image compressing and restoration.